Available online at www.sciencedirect.com

jmr&t Journal of Materials Research and Technology

journal homepage: www.elsevier.com/locate/jmrt

Investigating the effect of external force on the collision of an iron bullet with shear-thickening fluid nanocomposites using molecular dynamics simulation

Guoqi Guo [a], As'ad Alizadeh [b], Saeed Saber-Samandari [c,d,*], Maboud Hekmatifar [c,d,***], Jun Li [a,**], Mohammed Al-Bahrani [e], Navid Nasajpour-Esfahani [h], Mahmoud Shamsborhan [g], Davood Toghraie [f]

[a] School of Chemistry and Chemical Engineering, North University of China, Taiyuan 030051, People's Republic of China
[b] Department of Civil Engineering, College of Engineering, Cihan University-Erbil, Erbil, Iraq
[c] New Technologies Research Center, Amirkabir University of Technology, Tehran, Iran
[d] Composites Research Laboratory (CRLab), Amirkabir University of Technology, Tehran, Iran
[e] Chemical Engineering and Petroleum Industries Department, Al-Mustaqbal University College, Babylon, 51001, Iraq
[f] Department of Mechanical Engineering, Khomeinishahr Branch, Islamic Azad University, Khomeinishahr, Khomeinishahr, Iran
[g] Department of Mechanical Engineering, College of Engineering, University of Zakho, Zakho, Iraq
[h] Department of Material Science and Engineering, Georgia Institute of Technology, Atlanta 30332, USA

ARTICLE INFO

Article history:
Received 10 March 2023
Accepted 7 August 2023
Available online 11 August 2023

Keywords:
Iron bullet
Kevlar nanofibers
Silicon dioxide nanoparticles
Ethylene glycol
LAMMPS

ABSTRACT

The main uses of bullets are as projectiles in firearms for military, law enforcement, and civilian purposes. However, bullets have significant industrial applications beyond their role in weaponry, such as precision drilling, cutting, and shaping of hard materials. Steel bullets have a very resistant structure and will not be damaged if exposed to corrosion. Other applications that are resistant to strike and projectiles, such as the automotive and aerospace industries, are based on fibers or fabrics with high toughness and tensile strength, such as Kevlar and p -aramid fibers, which are impregnated with some thermoplastic or thermoset polymers. Therefore, in the upcoming research, the impact of external force (EF) with various values (0.1, 0.2, 0.3, 0.4, and 0.5 V/Å) on the strength of Kevlar nanofibers reinforced with silicon dioxide (SiO_2) nanoparticles and ethylene glycol (EG) has been investigated using LAMMPS software. EG and SiO_2 nanoparticles with 10 and 2 vol% were added to Kevlar fabrics, creating a shear thickening fluid (STF) nanocomposite. The energy parameters of the interaction between the particles, collision velocity, and the center of mass have been calculated. The findings of the research indicate an increase in the interaction energy from 111271.85 to 154351.15 kcal/mol, an increase in the collision

* Corresponding author. Composites Research Laboratory (CRLab), Amirkabir University of Technology, Tehran, Iran.
** Corresponding author.
*** Corresponding author. Composites Research Laboratory (CRLab), Amirkabir University of Technology, Tehran, Iran.
E-mail addresses: maboud.hekmatifar@iaukhsh.ac.ir (M. Hekmatifar), lijun2015@nuc.edu.cn (J. Li).
https://doi.org/10.1016/j.jmrt.2023.08.064

velocity from 0.7046 to 1.5812 Å/fs and an increase in the center of mass from 0.62671 to 1.1670 Å due to the EF applied from 0.2 to 0.4 (kcal/mol)/Å. These results show EF should be optimized in actual cases for the collision process to occur effectively.

1. Introduction

Fiber-reinforced polymer (FRP) composites are materials of a polymer matrix reinforced with fibers. These fibers can be made of various materials, including glass, carbon, or aramid. Composites are known for their high strength-to-weight ratio, corrosion resistance, and durability, making them useful in various applications, from aerospace to construction [1–7]. In ancient times, people protected themselves from harm with various materials. Later, they developed a bulletproof vest that protects against critical internal injuries caused by bullets. Today, Kevlar fibers are considered one of the most widely used aramid fibers due to their high strength to light weight ratio. Although Kevlar is a better material for this application, the vest wearer must absorb the bullet's energy, causing severe damage and blunt force trauma. Only many layers of Kevlar can protect the wearer, which increases the weight of the armor. It also does not protect against other injuries such as knives or sharp objects. Nowadays, nano reinforcements act as materials with many applications in various fields. High strength, lightweight, and excellent energy absorption properties make them suitable materials for military applications. Kevlar nanofibers can be reinforced with silicon dioxide (SiO_2) nanoparticles and ethylene glycol (EG) to create a shear-thickening fluid (STF) nanocomposite. This type of nanocomposite has unique properties, such as changing from a liquid to a solid-like state when subjected to mechanical stress [8]. This makes STF nanocomposites useful in various applications, such as body armor, protective gear, and impact-resistant coatings [9]. Adding SiO_2 nanoparticles and EG to Kevlar nanofibers enhances the mechanical properties of the resulting STF nanocomposite, making it stronger and more durable.

So far, many researchers have focused on Kevlar nanofibers reinforced with different nanoparticles due to their desirable properties [10–13]. For instance, Sun et al. [14] evaluated high-strength, lightweight Kevlar-reinforced graphene oxide architectures. The purpose of this study was to investigate the mechanical properties and durability of these devices in specific conditions. The researchers subjected these devices to two different tests: (i) an impact test with a force of 9.1 N caused by the fall of a metal ball; and (ii) a bending test with deformation up to 90°. It is worth noting that the devices did not change during these tests and remained untouched. The findings of this study show that the combination of hydrogel/Kevlar and reduced graphene oxide fabric in these symmetric gel-state devices provides a strong and durable material with potential applications in fields where resistance to mechanical stresses and shocks is essential. Wang et al. [15] fabricated an enhanced Kevlar-based triboelectric nanogenerator (EK-TENG) with excellent protection and stable sensing capability in harsh loading environments with graphene on Kevlar fabric. The results showed that the anti-ballistic EK-TENG could withstand a bullet of 126.6 m/s, higher than the 90.1 m/s of regular Kevlar. Amirian et al. [16] experimentally and numerically investigated Kevlar-basalt hybrid composites' high-velocity impact (HVI) behavior based on epoxy. The results showed that the hybridization improves the behavior of the composites in high-velocity impacts compared to the non-hybridized samples. Pandya et al. [17] compared the ballistic impact behavior of T- 300 Carbon/Epoxy composite with E-glass/Epoxy composite. Results showed that the E-glass/epoxy specimen had a higher ballistic limit velocity than the T-300 carbon/epoxy specimen. Parameters such as projectile shape, velocity, and target thickness were kept constant. Elazab [18] examined the strength of reinforced nanocomposite of Kevlar/epoxy. The results showed that reinforcing fabrics adds more strength to fabrics instead of using several non-reinforced fabrics. This increases the weight, thickness and reduces the cost of the final product.

According to the results obtained from the previous section, no study has been done on the effect of the force of the iron ball on the strength of Kevlar nanofibers using molecular dynamics (MD) simulation. In the present study, the simulated Kevlar nanofibers were reinforced with SiO_2 nanoparticles and EG using LAMMPS software based on MD concepts in the present study. EG and SiO_2 nanoparticles with a 10 and 2 vol% fraction were added to Kevlar fabrics, creating an STF nanocomposite. The use of MD simulation to model the behavior of FRP composites provides the ability for researchers to gain insights into how the individual components of the material interact with each other and how these interactions affect the overall mechanical properties of the material in future research. This can help guide the development of new FRP composites with improved performance characteristics.

2. The MD simulation approach

2.1. *Basic concepts and formulations*

One of the most important and accurate simulation methods is the MD. The MD simulation is one of the computational branches of physics and can describe and simulate the interaction between particles in time intervals based on the laws of physics. This method was first used in 1959 by Alder and Wainwright [19] based on the hard-sphere model. By the MD simulation, many properties of the whole system can be understood according to the structure and interactions of the constituent atoms or molecules. Newton's equations of motion are one of the basic equations that are the basis of the MD

Table 1 – LJ potential function parameters of particles in MD simulation based on selective force field [29,30].

Particles	σ (Å)	ε (kcal/mol)
H	2.886	0.044
N	3.6660	0.069
C	3.851	0.105
O	3.710	0.4150
Si	3.69	0.0043

simulation method. By solving these equations for the particles that make up the system, the movement path of all the particles can be simulated over time. The force acting on particle i can be expressed as follows through the potential function [20]:

$$F_i = m_i a_i = -\nabla_i U = -\frac{dU}{dr_i} \tag{1}$$

In Eq. (1), m_i is the mass of the i_{th} particle. Acceleration is also obtained from the following relationship [20]:

$$a_i = \frac{d^2 r_i}{dt^2} \tag{2}$$

From the combination of Eqs. (1) and (2), the position of the particles is obtained using the potential function [20]:

$$-\frac{dU}{dr_i} = m_i \frac{d^2 r_i}{dt^2} \tag{3}$$

In this method, the analytical description of particle motion is difficult and sometimes impossible because the force acting on a particle depends on its position relative to other particles. For this reason, integral algorithms should be used to solve the equations of motion. The velocity-Verlet algorithm is a valuable numerical integration technique developed from the finite difference method. Its main application lies in solving Newton's equations of motion, making it an essential tool in MD simulation, computational physics, and other fields where the dynamic behavior of particles and systems must be accurately and efficiently simulated over time [21,22]. In this method, the total simulation time is converted into very small times, the integration calculations are performed in very small and equal intervals, and the force will be obtained as a total of the interactions of the particle with the surrounding particles in equal and small time intervals. The velocity-Verlet algorithm is applied in LAMMPS software according to Eqs. (4) and (5) [21,22]:

$$r_i\,(t+\Delta t) = 2\,r_i(t) - r_i(t-\Delta t) + \left(\frac{d^2 r_i}{dt^2}\right)(\Delta t)^2 \tag{4}$$

$$v_i(t) = \frac{r_i\,(t+\Delta t) - r_i(t-\Delta t)}{2\Delta t} + d(\Delta t^2) \tag{5}$$

According to Eqs. (4) and (5), the final value of the position and velocity of the particles is calculated by having the initial position and velocity as well as the size of the time steps. The definition of the potential function and interparticle forces is one of the important factors in the MD simulations so that with a more accurate selection of the force field, the actual path taken in the physical process can be predicted more accurately. For this reason, the identification and selection of force fields and potential function are highly necessary. In this research, Lennard Jones (LJ) and Embedded Atom Method (EAM) potential functions have been utilized to describe the interaction between particles and metal particles [23,24]. Previous studies show that the LJ potential function defines the interaction between polymer structures well [25,26]. Also, the LJ potential can be used to model the nonbonded interactions between polymer chains and nanoparticles in polymer nanocomposites [27]. In the following, the mentioned potential functions will be discussed. The LJ potential function is expressed by Eq. (6) [28]:

$$U_{LJ} = 4\varepsilon_{ij}\left[\left(\frac{\sigma_{ij}}{r}\right)^{12} - \left(\frac{\sigma_{ij}}{r}\right)^{6}\right] \tag{6}$$

In Eq. (6), the epsilon defines the interaction well, and the sigma constant describes the distance at which the atomic interaction is zero, and r is the interatomic distance. The interaction between other particles in the simulation is described using Table 1 and Eqs. (7) and (8) [29].

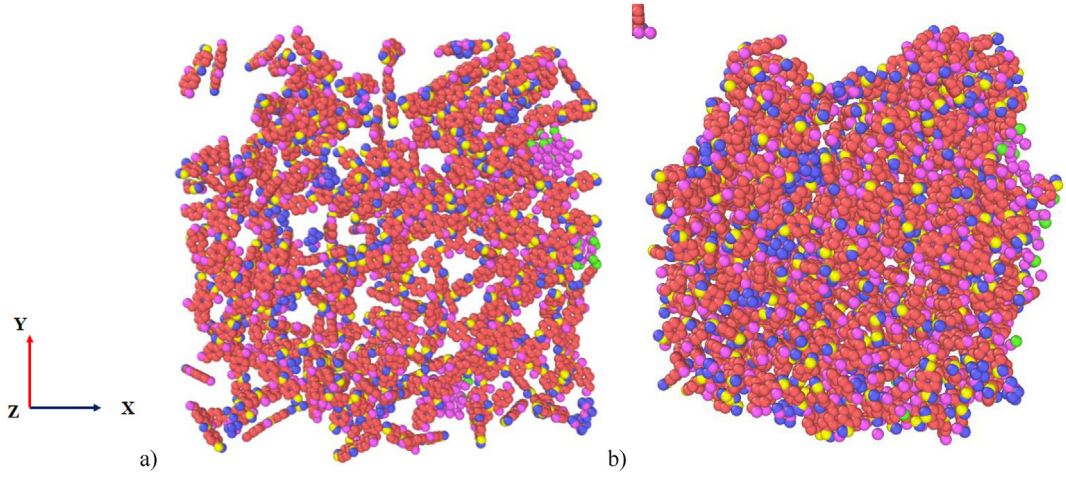

Fig. 1 – Overview of the simulated structure a) before and b) after equilibration.

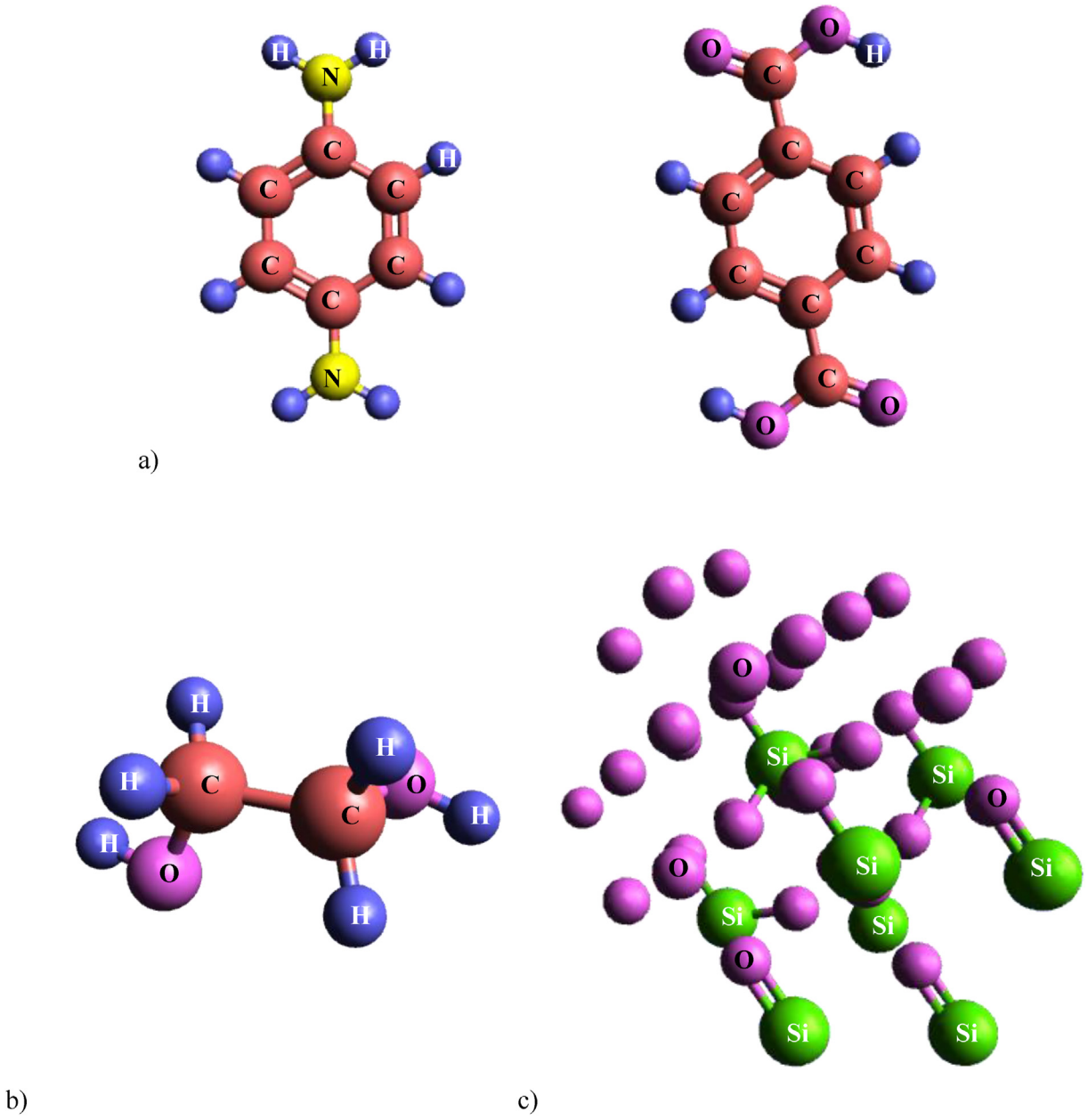

Fig. 2 – The chemical structure of the a) Kevlar fiber, b) EG, and c) SiO_2 nanostructures.

$$\varepsilon_{ij} = \sqrt{\varepsilon_i \varepsilon_j} \tag{7}$$

$$\sigma_{ij} = \frac{\sigma_i + \sigma_j}{2} \tag{8}$$

The EAM potential is a type of interatomic potential used in MD simulations to model metallic systems. The EAM potential has been used to study a wide range of metallic systems, including pure metals, alloys, and metallic surfaces [31,32]. The EAM potential introduced by Daw et al. [33] and Foiles et al. [34] is the most used potential function in the current study. The EAM is a multi-body potential function represented as follows:

$$U_i = \sum_{i=1}^{N-1} \sum_{j=i+1}^{N} \varphi(r_{ij}) + \sum_{i=1}^{N} F(\rho_i) \tag{9}$$

$$\rho_i = \sum_{i=1}^{N} \psi(r_{ij}) \tag{10}$$

In which i and j are the interacting atoms among N atoms with the distance of r_{ij}. $\Phi(r_{ij})$ and $F(\rho_i)$ are the interatomic energy and potential embedding function, respectively.

2.2. *Simulation details*

The current work evaluated the iron bullet's external force (EF) effect on the STF nanocomposite resistance during collision using MD simulation. First, Kevlar fiber is modeled utilizing Avogadro software. Next, to model the STF, nanocomposites, EG, and SiO_2 nanoparticles were modeled using Avogadro

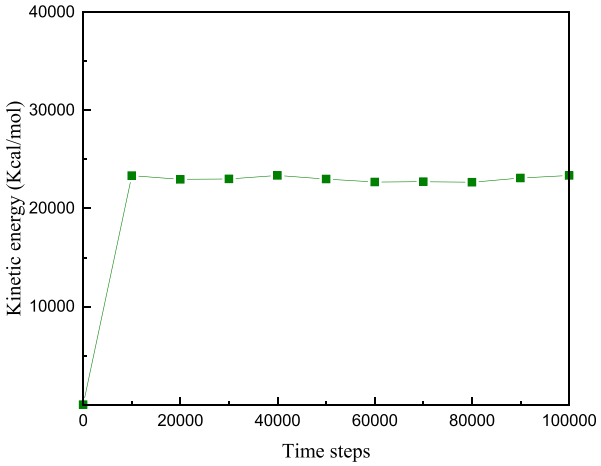

Fig. 3 – KE alterations of the investigated structure vs. time step.

software and with 10 and 2 vol% were added to the initial Kevlar structure. These atomic structures are packed utilizing Packmol software. The number of simulated particles in the upcoming work is 5160 atoms. The dimension of the simulation box is considered 110 Å in all directions. The boundary conditions considered for investigating the desired structure are periodically in the X and Y directions and fixed in the Z direction. Next, an iron bullet is modeled with a radius of 7 Å using LAMMPS software. The number of iron particles in the simulation box is 117 atoms. This study investigated the effect of the speed of the iron ball on the strength of the STF nanocomposite. When an iron bullet collides with STF nanocomposites, the outcome depends on various factors, such as the speed and force of the collision. STF nanocomposites are generally designed to absorb and disperse energy, so the iron bullet would likely experience some resistance when colliding. The STF nanocomposites would stretch and deform under the impact force, absorbing some energy and reducing the impact force on the other side of the material. However, the STF nanocomposites could break or tear if the collision is forceful enough, allowing the iron bullet to pass through. The initial temperature was set to 300 K using the NVT (Constant temperature, constant volume) ensemble. And the Nose-Hoover thermostat has been utilized to control temperature. After modeling the initial structure, the equilibration of simulated structures is checked with the change in kinetic energy (KE) and potential energy (PE). Fig. 1 shows the desired STF nanocomposite structure before and after the equilibrium process. And chemical structure of the Kevlar fiber, EG, and SiO_2 nanostructures is shown in Fig. 2. After making sure of the accuracy of the modeled structure, the iron bullet is thrown towards the STF nanocomposite with different speeds and the velocity of the moment of collision, the energy on the interaction between particles, and the distance of the center of mass by change is checked. To change the velocity of the iron bullet, an EF with magnitudes of 0.1–0.5 (kcal/mol)/Å is applied to it. In this step, the ensemble change from NVT to NVE (Constant energy, constant volume).

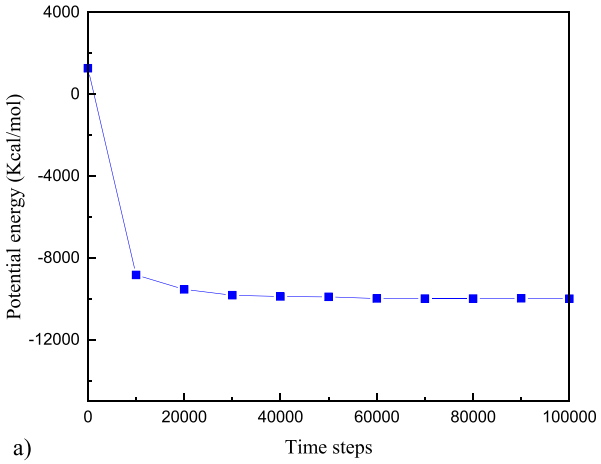

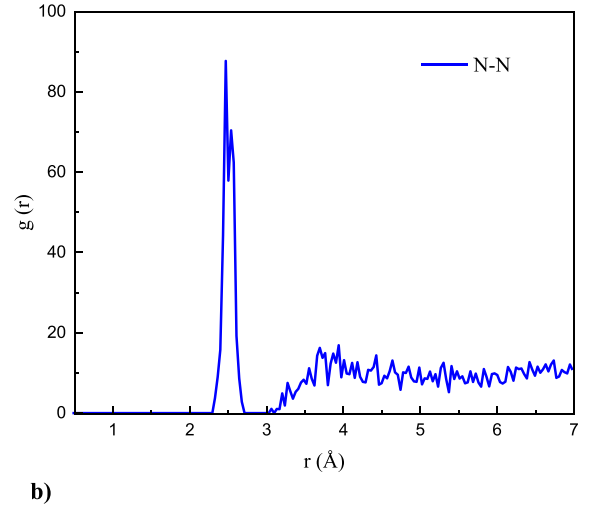

Fig. 4 – a) PE alterations of the investigated structure vs. time step. b) the RDF output of Kevlar (N–N) nanostructure after equilibrium phase detection.

3. Results and discussion

Before collision simulation in current research, the equilibrium process of the modeled sample was done for 100,000-

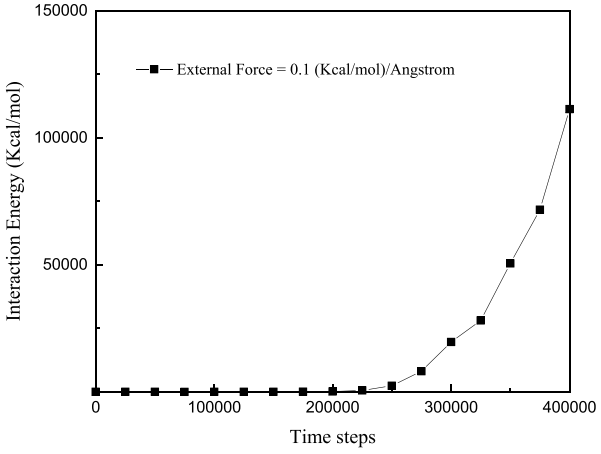

Fig. 5 – Alterations in the interaction energy in the desired nanocomposite vs. time step.

time steps. Here, the used thermostat decreased the atomic fluctuations to a constant value, and the physical stability of the modeled system can be concluded from this procedure. KE changes in this step are depicted in Fig. 3. Numerically, the KE converged to 23362.68 kcal/mol in the final time step of the equilibrium phase. This convergence arises from atomic mobility decreasing by simulation time passing. Furthermore, PE parameter changes as a function of simulation timesteps show similar behavior. This parameter converged to −9995.944 kcal/mol after equilibrium phase detection inside the MD box (Fig. 4). Physically, The balance established in repulsive and attractive forces between particles stabilizes the structure in an equilibrium position, which indicates the stability of the structure in the defined initial condition. This behavior is consistent with previous reports and shows appropriate settings in current research [35,36].

Also, to validate our computational approach in current research, the radial distribution function (RDF) of equilibrated nanocomposite calculate (see Fig. 4b). The RDF output is consistent with the previously reported atomic structure. It shows the correctness of our computational method in current research [37]. Furthermore, to show the adoption between the defined atomic model and the used force field, the center of mass of the matrix in the initial and final time steps of this section is calculated. Numerically, the center of masses of the nanocomposite samples are 54.26, 53.08, 10.16 Å as well as 57.52, 46.20,17.39 Å, in the initial and final steps, respectively. From these outputs, it was concluded that the nanocomposite's center of mass does not diverge with time steps passing.

Before simulating an impact, it is important ensuring that the iron bullet size is appropriate. For this purpose, the interaction energy between bullet atoms and matrix atoms (separately) was measured. MD approach predicted a magnitude of 3.28 and 2.90 kcal/mol for these parameters, respectively. The comparability of these interaction energies predicted the effective atomic evolution of nanocomposite after an iron bullet collided with this structure.

In this section, the interaction energy of the simulated particles has been evaluated in 400,000-time steps by applying an EF of 0.1 (kcal/mol)/Å. Interaction energy changes can be described as collision phenomena. As shown in Fig. 5, the interaction energy converged to a larger ratio by collision inside the simulation box. This process arises from atoms' distance decreasing between modeled parts. By decreasing interatomic distance, the system's energy enlarged and reached 111271.85 kcal/mol after 400,000-time steps. This energy enlarging predicted mutual interaction between the bullet and STF-based nanocomposite.

Also, the velocity of the bullet followed a similar pattern. As shown in Fig. 6, the bullet's velocity increases, and this procedure shows an effective collision process. It can be said that the fluctuation of this quantity over time indicated structural fluctuations in the sample. Numerically, this physical parameter converged to 0.7046 Å/fs in the current computational step.

Distance between the center of mass of the bullet and STF-based nanocomposite addressed atomic collision in modeled samples with more details. Numerical outputs for this parameter are reported in Fig. 7. MD outputs predicted center of mass distance decreases by simulation time passing. This process shows bullet samples and pristine composite as separate systems approach each other. Physically, the attraction force enlarging against repulsive mutual force caused the bullet sample to diffuse inside the atomic matrix, and the center of mass distance difference decreased. After this diffusion, the repulsive force was created, and the center of mass difference increased to 0.62671 Å. These calculations predicted 400,000-time steps to fulfill the coalition phenomenon in the defined initial condition. The described collision process is depicted in Fig. 8.

EF, implemented to the bullet in the collision process, is an important parameter for this particle-base procedure. Fig. 9 shows that the interaction energy between the bullet and STF-based nanocomposite increased by EF enlarging and reached a maximum ratio of 0.4 (kcal/mol)/Å. This calculation predicted the collision process to occur effectively by using this EF. We expected the attraction force between two isolate samples to be maximized more efficiently using this EF and collision procedure. More enlarging of EF caused repulsive force between particles in various regions of modeled samples

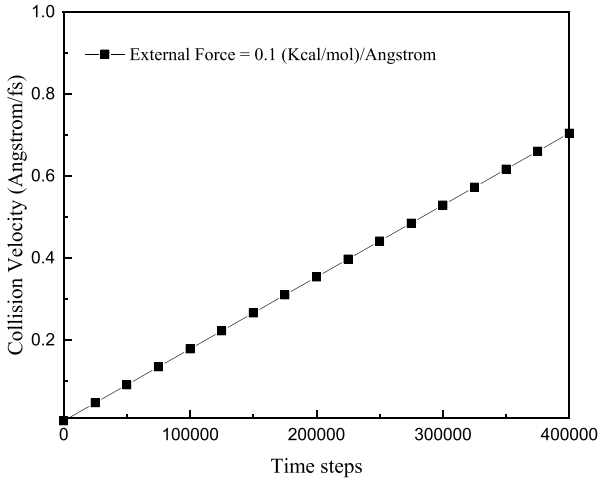

Fig. 6 – Alterations in the collision velocity in the desired nanocomposite vs. time step.

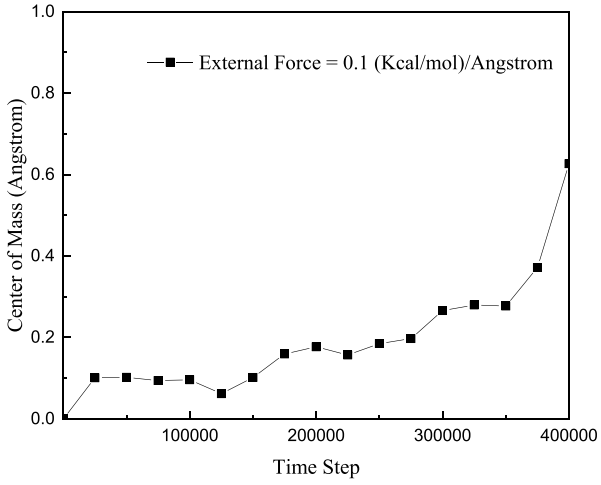

Fig. 7 – Alterations in the center of mass in the desired nanocomposite vs. time step.

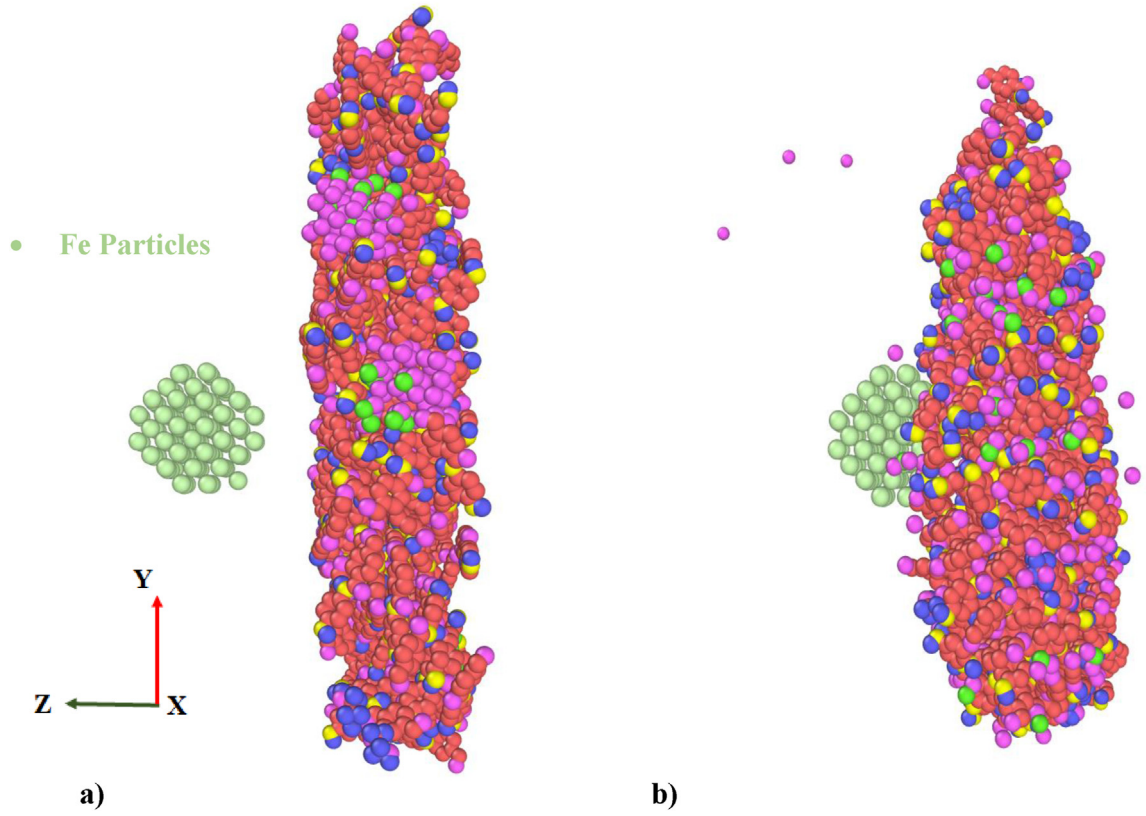

Fig. 8 – The desired STF nanocomposite a) before and b) after the impact of the iron bullet.

to be activated, and the diffusion process of the bullet inside the nanocomposite was disrupted. Structurally, this performance arises from interatomic distance decreasing between bullet particles and matrix, which arises from collision velocity enlarging as depicted in Fig. 9. The interaction energy and velocity in optimum condition converged to 154351.15 (kcal/mol)/Å and 1.5812 Å/fs, respectively.

Alterations in the collision velocity of the projectile on the nanocomposite due to the application of various EFs are presented in Fig. 10. The finding of this part demonstrates that the increase of EFs applied to the projectile leads to the increase of the projectile velocity. Therefore, the projectile hits the target with more energy and velocity. Moreover, the collision velocity of the iron bullet with the desired nanocomposite increases linearly with the increase of the force applied to the iron bullet. The numerical results are fully written in Table 2. Based on these results, by incrementing the force applied to the iron bullet from 0.2 to 0.5 (kcal/mol)/Å, the values related to the collision velocity have incremented from 1.1429 to 1.7565 Å/fs.

Fig. 11 shows the center of mass difference as a function of EF. As reported before, by using 0.4 (kcal/mol)/Å EF, the collision process occurred effectively, and the center of the mass

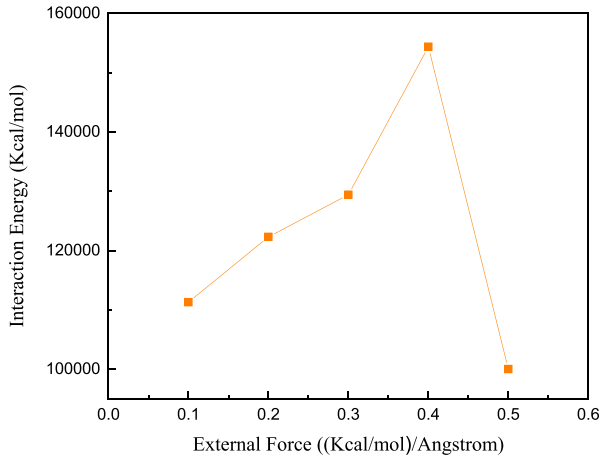

Fig. 9 – Alterations in the interaction energy vs various EF.

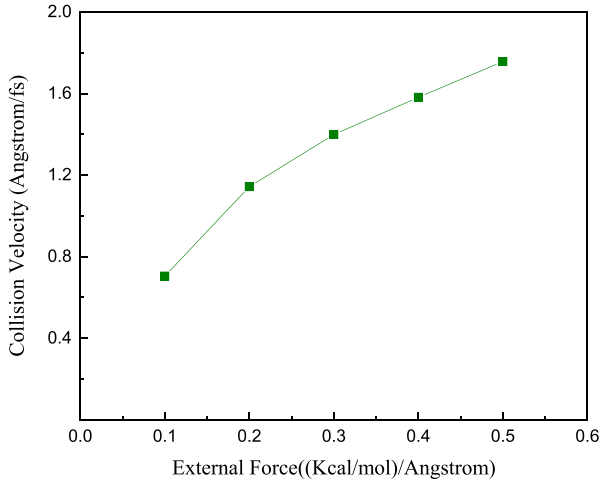

Fig. 10 – Alterations in the collision velocity vs. various EF.

Table 2 – The alterations of interaction energy parameters, collision velocity, and center of mass versus applied EF.

EF ((kcal/mol)/Å)	Interaction Energy (kcal/mol)	Collision Velocity (Å/fs)	Center of mass (Å)
0.1	111271.85	0.7046	0.62671
0.2	122303.52	1.1429	0.9327
0.3	129401.30	1.3989	0.9695
0.4	154351.15	1.5812	1.1670
0.5	100004.41	1.7565	0.2503

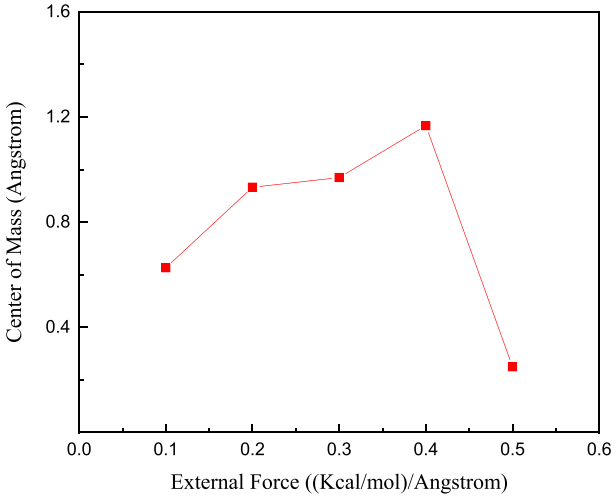

Fig. 11 – Alterations in the center of mass vs various EF.

difference between modeled matrix and bullet reached 1.167 Å. By increasing the EF, the collision process caused modeled matrix to penetrate and the pristine matrix to be destructed by MD time passing. So, optimization of EF in described simulation is necessary for the defined initial condition. In actual cases, we expected similar outputs. So, we concluded EF changes could be manipulated diffusion ratio of the metallic bullet inside an STF-based matrix and should be supposed in actual applications. Numerically, the center of mass difference changes from 0.62671 to 0.2503 Å by EF variation, as listed in Table 2.

4. Summary and conclusions

The present work evaluated the effects of the force applied to the iron bullet at the moment of collision with the nanocomposite. The force applied to the iron bullet was adjusted in various values (0.1, 0.2, 0.3, 0.4, and 0.5 ((kcal/mol)/Å)). The finding of the research was evaluated utilizing the MD simulation procedure. At first, the structure was balanced in the initial conditions and 100,000-time steps utilizing the NVT ensemble. In another step, after 400,000-time steps, the energy parameters of the interaction, the collision velocity of the iron bullet on the target nanocomposite, and the center of mass of the particles were determined utilizing the NVE ensemble. The results are summarized below.

- The finding of this article demonstrates that the KE of the desired structure has approached a specific number (23362.68 kcal/mol) after the 100,000-time step.
- The results demonstrate that the PE quantity reaches the value of −9995.944 kcal/mol after the 100,000-time step. The negative sign is due to the attendance of an attractive force between the particles, and this force causes the particles to be close to each other in the simulation.
- By applying an EF of 0.1 (kcal/mol)/Å to the iron bullet, the nanoparticles are compressed together and lead to a quantity of interaction energy reaching the value of 111,271.85 kcal/mol in the 400,000-time step.
- By increasing the time step to 400,000 and introducing an EF of 0.1 (kcal/mol)/Å to the projectile, the velocity alterations at the moment of collision have incremented linearly.
- By applying a force of 0.1 (kcal/mol)/Å to the iron bullet and incrementing the time step, the distance of the center of mass of the particles increments to 0.62671 Å.
- When the EF applied to the iron bullet reaches from 0.2 to 0.4 (kcal/mol)/Å, the amount of interaction energy increases from 122303.52 to 154351.15 kcal/mol, and then by applying more EF (0.5 (kcal/mol)/Å), this value decreases to 100004.41 kcal/mol.
- When the EF applied to the iron bullet reaches from 0.2 to 0.5 (kcal/mol)/Å, the collision velocity of the iron bullet on the STF nanocomposite increments linearly from 1.1429 to 1.7565 Å/fs.
- When the EF applied to the iron bullet reaches from 0.2 to 0.4 (kcal/mol)/Å, the distance of the center of mass reaches from 0.9327 to 1.1670 Å and then by applying a larger EF (0.5 (kcal/mol)/Å), the mentioned parameter is reduced to 0.2503 Å.

Declaration of competing interest

The authors declare that they have no known competing financial interests or personal relationships that could have appeared to influence the work reported in this paper.

Acknowledgement

This work was sponsored in part by Shanxi Scholarship Council of China (2020-107).

REFERENCES

[1] Yu H, Zhu J, Qiao R, Zhao N, Zhao M, Kong L. Facile Preparation and Controllable Absorption of a Composite Based on PMo12/Ag Nanoparticles: Photodegradation Activity and Mechanism. ChemistrySelect 2022;7(2):e202103668.

[2] Su Z, Meng J, Su Y. Application of SiO_2 nanocomposite ferroelectric material in preparation of trampoline net for physical exercise. Adv Nano Res 2023;14(4):355–62.
[3] Zhang W, Kang S, Liu X, Lin B, Huang Y. Experimental study of a composite beam externally bonded with a carbon fiber-reinforced plastic plate. J Build Eng 2023;71:106522.
[4] Zhao Y, Jing J, Chen L, Xu F, Hou H. Current research status of interface of ceramic-metal laminated composite material for armor protection. Jinshu Xuebao/Acta Metall Sin 2021;57:1107–25.
[5] Chen L, Zhao Y, Jing J, Hou H. Microstructural evolution in graphene nanoplatelets reinforced magnesium matrix composites fabricated through thixomolding process. J Alloys Compd 2023;940:168824.
[6] Zhang G, Chen J, Zhang Z, Sun M, Yu Y, Wang J, et al. A novel parametric model for nonlinear hysteretic behaviours with strain-stiffening of magnetorheological gel composite. Compos Struct 2023;318:117082.
[7] Yang K, Wu Z, Zhou C, Cai S, Wu Z, Tian W, et al. Comparison of toughening mechanisms in natural silk-reinforced composites with three epoxy resin matrices. Compos Appl Sci Manuf 2022;154:106760.
[8] Ghosh A, Majumdar A, Butola BS. Rheometry of novel shear thickening fluid and its application for improving the impact energy absorption of p-aramid fabric. Thin-Walled Struct 2020;155:106954.
[9] Wei M, Lin K, Sun L. Shear thickening fluids and their applications. Mater Des 2022:110570.
[10] Wang F, Wu Y, Huang Y, Liu L. Strong, transparent and flexible aramid nanofiber/POSS hybrid organic/inorganic nanocomposite membranes. Compos Sci Technol 2018/03/01;156:269–75. https://doi.org/10.1016/j.compscitech.2018.01.016. 2018.
[11] Mourad AHI, Cherupurakal N, Hafeez F, BarsoumImad I, GenenaFarah A, Genena FA, et al. Impact strengthening of laminated kevlar/epoxy composites by nanoparticle reinforcement. Polym 2020;12(12):2814.
[12] Yadav PS, Purohit R, Namdev A. Physical and mechanical properties of hybrid composites using Kevlar fibre and nano-SiO2. Advances in Materials and Processing Technologies 2022/11/30;8(sup4):2057–69. https://doi.org/10.1080/2374068X.2022.2034312. 2022.
[13] Venkataraman M, Xiong X, Novotná J, Kašparová M, Mishra R, Militký J. Thermal protective properties of aerogel-coated Kevlar woven fabrics, 12; 2019. p. 93–101.
[14] Sun W, Shah SA, Lowery JL, Oh JH, Lutkenhaus JL, Green MJ. Lightweight kevlar-reinforced graphene oxide architectures with high strength for energy storage. Adv Mater Interfac 2019/11/01;6(21):1900786. https://doi.org/10.1002/admi.201900786. 2019.
[15] Wang W, Jianyu Z, Sheng W, Fang Y, Shuai L, Junshuo Z, et al. Enhanced Kevlar-based triboelectric nanogenerator with anti-impact and sensing performance towards wireless alarm system. Nano Energy 2022/01/01;91:106657. https://doi.org/10.1016/j.nanoen.2021.106657. 2022.
[16] Amirian A, Rahmani H, Moeinkhah H. An experimental and numerical study of epoxy-based Kevlar-basalt hybrid composites under high velocity impact. J Ind Text 2022;51(1_suppl):804S–21S.
[17] Pandya KS, Pothnis JR, Ravikumar G, Naik NK. Ballistic impact behavior of hybrid composites. Mater Des 2013/02/01;44:128–35. https://doi.org/10.1016/j.matdes.2012.07.044. 2013.
[18] Elazab Dr HA. Bulletproof vests/shields prepared from composite material based on strong polyamide fibers and epoxy resin. 2017.
[19] Alder BJ, Wainwright TE. Studies in molecular dynamics. I. General method. J Chem Phys 1959;31(2):459–66.
[20] Rapaport DC, Rapaport DCR. The art of molecular dynamics simulation. Cambridge university press; 2004.
[21] Zhang L, Xiong D, Su Z, Li J, Yin L, Yao Z, et al. Molecular dynamics simulation and experimental study of tin growth in SAC lead-free microsolder joints under thermo-mechanical-electrical coupling. Mater Today Commun 2022;33:104301. https://doi.org/10.1016/j.mtcomm.2022.104301.
[22] Gao S, Wang H, Huang H, Kang R. Molecular simulation of the plastic deformation and crack formation in single grit grinding of 4H-SiC single crystal. Int J Mech Sci 2023;247:108147.
[23] Lennard-Jones JE. Cohesion 1931;43(5):461.
[24] Rappé AK, Casewit CJ, Colwell K, Goddard III WA, Skiff WM. UFF, a full periodic table force field for molecular mechanics and molecular dynamics simulations. J Am Chem Soc 1992;114(25):10024–35.
[25] Buell S, Van Vliet KJ, Rutledge GC. Mechanical properties of glassy polyethylene nanofibers via molecular dynamics simulations. Macromolecules 2009;42(13):4887–95.
[26] Yuan L, Shan D, Guo B. Molecular dynamics simulation of tensile deformation of nano-single crystal aluminum. J Mater Process Technol 2007/04/12;184(1):1–5. https://doi.org/10.1016/j.jmatprotec.2006.10.042. 2007.
[27] Chao H, Riggleman RA. Effect of particle size and grafting density on the mechanical properties of polymer nanocomposites. Polym 2013;54(19):5222–9.
[28] Lennard-Jones JE. Cohesion. Proc Phys Soc 1931;43(5):461.
[29] Rappé AK, Casewit CJ, Colwell K, Goddard III WA, Skiff WM. UFF, a full periodic table force field for molecular mechanics and molecular dynamics simulations. J Am Chem Soc 1992;114(25):10024–35.
[30] Mayo SL, Olafson BD, Goddard WA. DREIDING: a generic force field for molecular simulations. J Phys Chem 1990;94(26):8897–909.
[31] Alavi A, Mirabbaszadeh K, Nayebi P, Zaminpayma E. Molecular dynamics simulation of mechanical properties of Ni–Al nanowires. Comput Mater Sci 2010/11/01;50(1):10–4. https://doi.org/10.1016/j.commatsci.2010.06.037. 2010.
[32] Daw MS, Baskes MI. Embedded-atom method: derivation and application to impurities, surfaces, and other defects in metals. Phys Rev B 1984;29(12):6443–53. https://doi.org/10.1103/PhysRevB.29.6443. 06/15.
[33] Daw MS, Foiles SM, Baskes MI. The embedded-atom method: a review of theory and applications. Mater Sci Rep 1993;9(7–8):251–310.
[34] Foiles S, Baskes M, Daw MS. Embedded-atom-method functions for the fcc metals Cu, Ag, Au, Ni, Pd, Pt, and their alloys. Phys Rev B 1986;33(12):7983.
[35] Jolfaei NA, Jolfaei NA, Hekmatifar M, Piranfar A, Toghraie D, Sabetvand R, et al. Investigation of thermal properties of DNA structure with precise atomic arrangement via equilibrium and non-equilibrium molecular dynamics approaches. Comput Methods Programs Biomed 2020;185:105169.
[36] Karimipour A, Karimipour A, Jolfaei NA, Hekmatifar M, Toghraie D, Sabetvand R, et al. Prediction of the interaction between HIV viruses and human serum albumin (HSA) molecules using an equilibrium dynamics simulation program for application in bio medical science. J Mol Liq 2020;318:113989.
[37] https://commonchemistry.cas.org/detail?cas_rn=24938-64-5.